Deep learning–based synthesis of hyperpolarized gas MRI ventilation from 3D multi-inflation proton MRI

Joshua R. Astley[1] JASTLEY1@SHEFFIELD.AC.UK
[1] *POLARIS, The University of Sheffield, Sheffield, UK*
Alberto M. Biancardi[1] A.BIANCARDI@SHEFFIELD.AC.UK
Helen Marshall[1] H.MARSHALL@SHEFFIELD.AC.UK
Laurie J. Smith[1] LAURIE.SMITH@SHEFFIELD.AC.UK
Paul J.C. Hughes[1] PAUL.HUGHES@SHEFFIELD.AC.UK
Guilhem J. Collier[1] G.J.COLLIER@SHEFFIELD.AC.UK
Matthew Q. Hatton[1] MATTHEWHATTON@NHS.NET
Jim M. Wild[1,2] J.M.WILD@SHEFFIELD.AC.UK
[2] *Insigneo Institute for in-silico Medicine, The University of Sheffield, Sheffield, UK*
Bilal A. Tahir[1,2] B.TAHIR@SHEFFIELD.AC.UK

Editors: Under Review for MIDL 2022

Abstract

Hyperpolarized (HP) gas MRI allows visualization and quantification of regional lung ventilation; however, there is limited clinical uptake due to the requirement for highly specialized equipment and exogenous contrast agents. Alternative, non-contrast, model-based proton (^{1}H)-MRI surrogates of ventilation, which correlate moderately with HP gas MRI, have been proposed. Recently, deep learning (DL)-based methods have been used for the synthesis of HP gas MRI from free-breathing ^{1}H-MRI for a single 2D section. Here, we developed and evaluated a multi-channel 3D DL method that combines modeling and data-driven approaches to synthesize HP gas MRI ventilation scans from multi-inflation ^{1}H-MRI.

Keywords: Deep learning, image synthesis, proton MRI, functional imaging

1. Introduction

Hyperpolarized (HP) gas MRI allows visualization and quantification of regional lung ventilation with high spatial and temporal resolution; however, there is limited clinical uptake due to the requirement for highly specialized equipment and exogenous contrast agents, such as xenon-129 (^{129}Xe). Alternative, non-contrast proton (^{1}H)-MRI–based surrogates of ventilation, which exhibit moderate spatial correlation with HP gas MRI, have been proposed (Tahir et al., 2021). Recently, deep learning (DL) using convolutional neural networks (CNNs) has shown promise for several lung image synthesis applications (Astley et al., 2020). For example, the synthesis of HP gas MRI from free-breathing ^{1}H-MRI for a single 2D coronal section over time, limiting volumetric information on regional ventilation, has been reported (Capaldi et al., 2020). Here, we developed and evaluated a multi-channel 3D CNN method that combines modeling and data-driven approaches to synthesize functional 3D HP gas MRI scans from structural multi-inflation ^{1}H-MRI without exogenous contrast.

2. Methods

The data set comprised 3D ^{1}H-MRI scans acquired at approximately total lung capacity (TLC) and residual volume (RV), and HP ^{129}Xe-MRI ventilation scans with corresponding ^{1}H-MRI acquired at functional residual capacity (FRC)+bag from 150 healthy participants and patients with numerous lung pathologies. TLC and RV ^{1}H-MRI scans were aligned using deformable image registration and subsequently registered to the spatial domain of ^{129}Xe-MRI via the corresponding ^{1}H-MRI FRC+bag scan. Model-based ^{1}H-MRI ventilation surrogates were computed from the aligned TLC and RV ^{1}H-MRI scans as described previously (Tahir et al., 2021). We used a 3D multi-channel VNet CNN (Milletari et al., 2016), which employed the aligned RV and TLC ^{1}H-MRI scans and the corresponding model-based ^{1}H-MRI ventilation scans as inputs to generate synthetic ^{129}Xe-MRI scans. A Huber loss function with a delta of 0.1, PReLU activation function, and ADAM optimization on patches of 192x192x48 voxels were used. A learning rate of 1x10^{-5} and decay of 0.0001 were used for 1750 epochs of training. Five-fold cross-validation was used, resulting in training and testing sets of 120 and 30 participants, respectively, for each fold. ^{1}H-MRI ventilation scans and DL-generated synthetic ventilation scans were median filtered with a radius of 3x3x1 to account for noise and registration errors. We evaluated the accuracy of the synthetic ventilation scans through comparison with ^{129}Xe-MRI scans using voxel-wise Spearman's rs, mean absolute error (MAE), and root mean square error (RMSE) across the lung parenchyma. Paired t-tests were used to assess significances of differences between the proposed DL approach and the conventional ^{1}H-MRI ventilation model.

3. Results and Discussion

Qualitative spatial agreement and Spearman's correlation between ^{129}Xe-MRI and DL synthetic ventilation as well as ^{1}H-MRI ventilation models for three cases are shown in Figure 1.

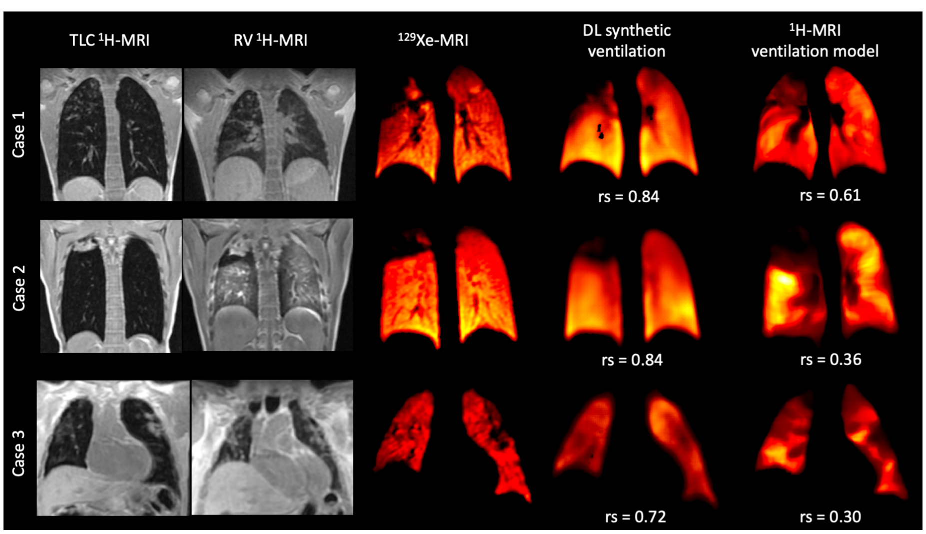

Figure 1: Example coronal slices of TLC and RV ^{1}H-MRI, ^{129}Xe-MRI, DL synthetic ventilation, and a conventional ^{1}H-MRI ventilation model for three random participants.

Table 1 displays results comparing the DL- and model-based ventilation methods; the DL method significantly outperformed the ^{1}H-MRI ventilation model ($p<0.0001$).

Table 1: Synthetic ventilation results from ^{1}H-MRI ventilation modeling and DL compared with ^{129}Xe-MRI ventilation. Median (range) values are provided.

Synthetic ventilation method	**Spearman's rs**	**MAE**	**RMSE**
^{1}H-MRI ventilation model	0.38 (–0.01, 0.61)	0.33 (0.09, 1.33)	0.41 (0.12, 1.50)
DL fold 1	0.68 (0.13, 0.85)	0.17 (0.07, 0.30)	0.20 (0.09, 0.32)
DL fold 2	0.66 (0.18, 0.84)	0.14 (0.07, 0.28)	0.18 (0.10, 0.31)
DL fold 3	0.67 (0.28, 0.79)	0.12 (0.09, 0.26)	0.16 (0.11, 0.30)
DL fold 4	0.69 (0.14, 0.83)	0.17 (0.07, 0.33)	0.20 (0.08, 0.35)
DL fold 5	0.66 (0.15, 0.84)	0.14 (0.08, 0.23)	0.17 (0.10, 0.28)
DL all folds	0.68 (0.13, 0.85)	0.14 (0.07, 0.33)	0.17 (0.08, 0.35)

Our study represents the first 3D synthesis of HP gas MRI from multi-inflation ^{1}H-MRI. The proposed DL-based multi-channel 3D CNN approach produced synthetic ventilation scans that mimicked HP gas MRI with good Spearman's correlation. Qualitative agreement, as shown in Figure 1, demonstrated the ability of synthetic functional MR images to mimic defects present in the corresponding ^{129}Xe-MRI scans. Cases 1 and 2 showed that gross ventilation defects present in the ^{129}Xe-MRI were replicated by the synthetic ventilation scans. This was further reinforced by the quantitative results showing significant improvements over conventional ^{1}H-MRI ventilation models.

Acknowledgments

We thank the patients from the NOVELTY study (funded by AstraZeneca, Cambridge, UK).

References

J. R. Astley, J. M. Wild, and B. A. Tahir. Deep learning in structural and functional lung image analysis. *Br J Radiol*, 0(0):20201107, 2020. doi: 10.1259/bjr.20201107.

D. P. I. Capaldi, F. Guo, L. Xing, and G. Parraga. Pulmonary ventilation maps generated with free-breathing proton MRI and a deep convolutional neural network. *Radiology*, 298 (2):427–438, 2020. ISSN 0033-8419. doi: 10.1148/radiol.2020202861.

F. Milletari, N. Navab, and S. A. Ahmadi. V-net: Fully convolutional neural networks for volumetric medical image segmentation. *Proceedings of 2016 Fourth International Conference on 3D Vision (3DV)*, pages 565–571, 2016. doi: 10.1109/3dv.2016.79.

B. A. Tahir, L. J. Smith, J. R. Astley, M. Walker, A. M. Biancardi, G. J. Collier, P. J. C. J Hughes, H. Marshall, and J. M. Wild. Proton lung ventilation mri in cystic fibrosis: comparison with hyperpolarized gas MRI, pulmonary function tests and multiple-breath washout. *Proceedings of 2021 ISMRM and SMRT Annual Meeting*, (3220), 2021.